



The Use of Mineral Magnetic Parameters to Characterize Archaeological Ochres

S. D. Mooney

School of Biological, Earth & Environmental Sciences, University of New South Wales, Sydney, NSW 2052, Australia

C. Geiss

Institute of Rock Magnetism, University of Minnesota, Minneapolis, MN 55455, U.S.A.

M. A. Smith

National Museum of Australia, GPO Box 1901, Canberra, ACT 2601, Australia

(Received 25 January 2001, revised manuscript accepted 24 May 2002)

The application of several magnetic parameters to ochre samples has found that they can be used to characterize samples from known ochre quarries. This technique also allows the sourcing of ochre found in archaeological contexts and provides an alternative to geochemical methods of provenancing ochres. Simple magnetic parameters (susceptibility and isothermal remanence) are effective in discriminating between ochre sourced from various quarries, however more sophisticated parameters are required to ascribe unknown samples to specific sources.

© 2002 Elsevier Science Ltd. All rights reserved.

Keywords: ENVIRONMENTAL MAGNETISM, OCHRE, PROVENANCE, CENTRAL AUSTRALIA.

Introduction

Mineral magnetics are most commonly applied to sediments for core correlation or to characterize the history of erosion (e.g. Thompson *et al.*, 1975; Dearing & Flower, 1982). Magnetic parameters have also been successfully applied to other palaeoenvironmental studies including investigation of fire history (Rummary, 1983), the consequences of changes in human economies/land-use (e.g. Oldfield, 1988), climate change and pedogenesis (e.g. Zhou *et al.*, 1990; Maher & Thompson, 1992) and the history of particulate pollution (Oldfield *et al.*, 1981). The most familiar application of mineral magnetics in archaeology is in site prospecting and surveys (Thompson & Oldfield, 1986). This commonly includes the identification of magnetically enhanced materials associated with heating such as hearths and kilns.

The monograph *Environmental Magnetism* (Thompson & Oldfield, 1986: 200) concluded that

“there are few aspects of Quaternary studies that cannot benefit from mineral magnetic measurements”. Many in the field have also highlighted the relative speed in which interpretable magnetic measurements are obtainable, however, Oldfield (1991) saw more virtue in the capacity of mineral magnetics to address problems that were inaccessible to pre-existing techniques.

In Australia there have been several attempts to characterize ochres on the basis of their mineralogy and geochemistry (Clarke, 1976; Clarke & North, 1991; David *et al.*, 1993, 1995; Sagona, 1994; Goodall *et al.*, 1996; Smith & Fankhauser, 1996; Smith & Pell, 1997). Much of this research aims to characterize regional ochre sources with a view to provenancing the ochre found in archaeological sites or in rock paintings. This may hence provide new insights into patterns of change and continuity in prehistoric exchange networks and other forms of regional interactions. Satisfactory results appear to be obtained by using trace element chemistry together with mineralogy to characterize ochre sources (Smith & Fankhauser, 1996) and to provenance unknown ochres recovered from archaeological contexts (Smith *et al.*, 1998). Such

Corresponding author: Scott Mooney, School of Biological, Earth & Environmental Sciences, University of New South Wales, UNSW, NSW 2052, Australia. Tel.: +61 2 9385 4389; Fax: +61 2 9313 7878; Email: s.mooney@unsw.edu.au

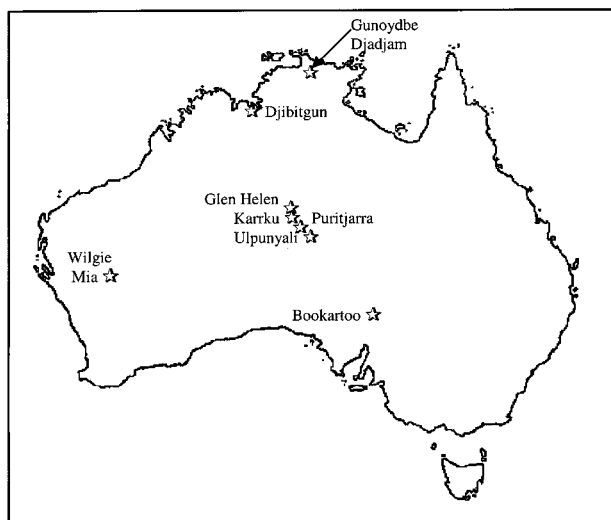


Figure 1. Locations mentioned in the text.

research, however, is still at an early stage of development and there are advantages in testing a range of alternative techniques.

Magnetic measurements are relatively simple and non-destructive and because of this may have practical advantages over other techniques. In this paper we assess the utility of a number of magnetic parameters in characterizing a series of ochre samples. This study complements that by [Smith & Pell \(1997\)](#) who attempted to characterize the same samples using $\delta^{18}\text{O}$ content of quartz clasts in the ochre.

Materials

The materials used in this study consist of samples of raw ochre collected from various Australian sources, mainly in central Australia ([Figure 1](#)). None of the samples have been prepared as a pigment or paint and none have been burnt. The latter is important as heating ochre in a reducing atmosphere (wood fire) could alter their magnetic properties through dehydration, reduction or alteration of the crystalline properties.

We have deliberately included ochres with a range of properties in order to test the utility of the method. As magnetic properties are largely related to iron-rich minerals we included samples that allow us to compare Fe-rich and Fe-poor ochres. We also included both red (hematite) and yellow (goethite) ochres in order to compare ochres which differ in the dominant iron mineral present. Samples from different parts of one source, the Karrku ochre seam (see below), are included to test whether significant intra-source variability in magnetic characteristics occurs. Two ochres of unknown provenance were also included in the experiment to test the ability of the method to determine possible sources. To test if the sediment matrix could be distinguishable from ochre found in this matrix we

also analysed a sample of sediment from the Puritjarra excavations.

Further descriptions of the samples used in this study and the details of their chemistry and mineralogy can be found in [Smith & Fankhauser \(1996\)](#).

Ochre sources

Ulpunyali. Ulpunyali is an important red ochre quarry, west of Kings Canyon, in Central Australia. Three samples were tested from this quarry, all from the same large (~1 kg) block of ochre (Ulpunyali MAS). Two were of loosely cemented raw ochre, while the third sample (Ulpunyali no. 1) was the remaining portion of a sample which had been ground in preparation for SEM/EDXA analysis in 1988.

Ulpunyali ochre is coarse-grained with large rounded quartz grains set in a ferruginous cement. Iron content (assumed to be Fe_2O_3) varied from 20.5–50.7% in duplicate ochre samples analysed using SEM/EDXA ([Smith & Fankhauser, 1996](#)), in reverse proportion to the density of the quartz clasts in these samples. Analysis of mineralogy using Rietveld powder XRD techniques indicates this ochre consists of hematite (36.5%), goethite (5.8%), quartz (37.4%) and kaolinite (0.7%) with non-crystalline material making up 19.6%.

Bookartoo (also known as Pukartu). Bookartoo is another well-known source of red ochre, located in the northern Flinders Ranges, South Australia. [Keeling \(1984\)](#) reported that the ochre from Bookartoo is an earthy hematite infilling joints and fractures in dolomite. Analysis of the mineralogy of this ochre shows the following crystalline components: hematite (37.3%), quartz (7.8%), calcite (4.2%), dolomite (6.8%), ankerite (2.6%) and halite (0.9%). SEM/EDXA analysis of the sample tested here (Bookartoo MAS) shows it to have an iron content (Fe_2O_3) of 53.7%, which is towards the lower end of the recorded range for this ochre (51.9–92.6%).

Karrku no. 6. Karrku is a major red ochre mine in the Campbell Ranges in the western part of Central Australia ([Peterson & Lampert, 1985](#)). The ochre deposit forms a sub-horizontal seam between beds of orthoquartzite, basal pebbly haematic sandstone and conglomerate. Analysis of the mineralogy shows this ochre consists of hematite (39.5%), quartz (24.9%), muscovite (20.4%) and kaolinite (2.5%), with 12.7% of amorphous non-crystalline material. SEM/EDXA analysis of the three sample tested here (Karrku no. 6, Karrku 96/1 and 96/2) show them to have an iron content (Fe_2O_3) of 46.1%, 17.0% and 5.7% respectively. The three samples were from different parts of the ochre seam and have noticeable differences in concentration of quartz clasts.

Gunoydbe djadjam. This is a bed of friable earthy hematite located near the mouth of Deaf Adder Gorge,

in western Arnhem Land. The ochre is a reddish brown in colour (2.5YR 4/6 using [Munsell, 1994](#)). SEM/EDXA analysis of the sample tested here (Deaf Adder no. 5) shows it to have an iron content (Fe_2O_3) of 22.4%.

Djibitgun. Djibitgun is an ochre sourced from a quarry near the Jinmium site ([Fullager et al., 1996](#)), in the Keep River region of the Northern Territory. The Djibitgun ochre analysed here (Djibitgun 95/1) is a deep rich dark red colour (10R 3/6 using [Munsell, 1994](#)). Iron content, using SEM/EDXA, and assuming this in the form of Fe_2O_3 is 59.7%.

Wilgi Mia. Wilgi Mia in the Weld Range, Western Australia, is renowned for the large scale of the ethnographic excavations and the great quantity of red ochre removed at this site. [Davidson \(1952\)](#) thought that this quarry provided most of the red ochre used in the western part of Western Australia. According to [Elias \(1982\)](#) the Wilgie Mia deposit is formed in a large lens of jaspilite, characterized by red (hematite dust), white (silica) and black (magnetite) bands. [Clarke \(1976\)](#) reports that the ochre deposit is interbedded with argillaceous sediments. The sample tested in this study, Wilgie Mia N-2b, is a distinct purple colour (10R 2.5/2 using [Munsell, 1994](#)). Mineralogical analysis shows it to consist of hematite (60.0%), goethite (1.2%), calcite (2.6%) and dolomite (0.1%), with 36.1% amorphous material. SEM/EDXA analysis shows the iron content (Fe_2O_3) of this sample to be 97.1%, which is at the high end of the range for samples from this source (91.1–97.1%).

Puritjarra. Puritjarra rock shelter is a major archaeological site ([Smith, 1987; Smith et al., 1997](#)), situated in the Cleland Hills in western Central Australia. Sandstone formations in the vicinity of the rock shelter contain a thin layer of fine-grained friable yellow ferruginized sandstone. This material appears to have been utilized as pigment by prehistoric inhabitants of Puritjarra. The sample tested is a distinctly yellow material (10YR 7/8 using [Munsell, 1994](#)). SEM/EDXA analysis of a duplicate sample (Puritjarra yellow no. 8) indicates an iron content (Fe_2O_3) of 8.3%.

Glen Helen Ochre Pits. The Glen Helen source is a banded siltstone formation, exposed in a creek cutting in the foothills of the western MacDonnell Ranges, Central Australia. It is known locally as the “ochre pits” although little appears to be known about Aboriginal utilization of this source. Ochre from the site is a high-quality fine-grained homogenous yellow (2.5Y 7/8 in [Munsell, 1994](#)) ochre with a powdery texture. SEM/EDXA analysis indicates that the major constituent of this ochre is silt-sized quartz (SiO_2 content: 75.6%) with a comparatively low iron content (Fe_2O_3 content: 8.5%).

Other samples

Paterson X. Paterson X is a homogenous fine-grained purple-red ochre (10R 3/4; [Munsell, 1994](#)) obtained from an Aboriginal woman at Uluru in Central Australia. Although attributed by her to Ulpunyali, the chemistry and petrology of the sample rule out this possibility ([Smith & Fankhauser, 1996](#)). We believe the sample is derived from an alternative, local source in the nearby Petermann Ranges. Oxygen isotope ratios in quartz separates from this ochre also indicate that it cannot be from the same sedimentary basin as the Ulpunyali or Karrku ochres ([Smith & Pell, 1997](#)). SEM/EDXA analysis shows the iron content (Fe_2O_3) of this sample to be 51.3%.

Puritjarra N5/24-6. N5/24-6 is an archaeological ochre specimen from excavations at Puritjarra rock shelter ([Smith, 1987; Smith et al., 1997](#)). It is from a stratigraphic context dating to 13,000 BP and is representative of the red ochre found in late Pleistocene levels at this site. Trace element composition and mineralogy indicate that the analysed specimen, N5/24-6, is from the Karrku mine (see [Smith et al., 1998](#)). This attribution is also consistent with the findings of [Smith & Pell \(1997\)](#), although the oxygen isotope ratios do not discriminate between the Karrku and Ulpunyali sources.

N5/24-6 is a red ochre, to 10R 4/4 on the [Munsell \(1994\)](#) colour charts. The specimen is a single block of ochre and it is apparent that there are textural differences across the thickness of the piece. The proportion of quartz clasts increases towards the base of the piece, which appears to be orthoquartzite. This variability is reflected in successive SEM/EDXA analyses of the sample showing iron content (Fe_2O_3) varying from 31.6% to 17.3%. Mineralogical analysis shows that the major crystalline components of this ochre are hematite (10.0%), quartz (51.5%), muscovite (4.9%), kaolinite (12.8%) and anatase (0.6%), with 20.2% amorphous material.

Puritjarra sediment matrix. A sediment sample (N13-N-95, Puritjarra no. 10) from the excavations at Puritjarra rock shelter was also magnetically characterized, to test if the sediment matrix was distinguishable from the ochre found in this deposit. The sediment is a red silty sand with a similar colour to the red ochre samples ([Munsell, 1994: 2.5YR 4/8](#)). SEM/EDXA analysis shows that the iron content (Fe_2O_3) of the sample is 10.6%.

Methodology

Air-dried ochre samples were homogenized using a mortar and pestle and a known mass packed into clean Kartell plastic tubes (size 8.75 cm³) using pressure and cotton wool to ensure minimal movement of the ochre during measurements. The ochres were placed in the

Table 1. List of all magnetic parameters and their symbols used in this study

Magnetic parameter	Symbol	Interpretation
Magnetic susceptibility	χ (mass norm.) κ (vol. norm.)	Depends mainly on concentration of ferrimagnetic minerals (magnetite, maghemite), but is also function of magnetic particle size and magnetic mineralogy
Para- (dia)magnetic susceptibility	χ_P (χ_D)	Depends on presence and mineralogy of para- and diamagnetic minerals, such as Fe-bearing clays, quartz or calcite
Frequency dependent susceptibility	χ_{FD}	Indicator for the presence of ultra-fine ($d < 0.025 \mu\text{m}$) superparamagnetic (SP) particles
Isothermal remanent magnetization	IRM	Measures concentration of magnetic minerals, is also influenced by strength of applied field (which is often denoted by a subscript) and mineralogy of sample
Saturation isothermal remanent magnetization	SIRM	Maximum obtainable IRM, depends on concentration and particle size of magnetic minerals
Anhysteretic remanent magnetization	ARM	Measure of fine grained stable single domain (SSD) magnetic particles ($0.025 \mu\text{m} < d < 0.05 \mu\text{m}$), also sensitive to grain interactions
Saturation magnetization	M_s	Maximum obtainable magnetization while the sample is exposed to a magnetic field, depends on mineralogy and concentration of magnetic grains but is independent of particle size
Coercive force	B_C	Describes resistance of sample to a magnetic field, depends on magnetic mineralogy and particle size
S-ratio	S	Indicator for coercivity, depends on mineralogy, to a lesser degree on particle size

centre of the sample tubes, with cotton wool filling the upper and lower quarters, to ensure that they were in the approximate centre of all instrumentation.

Multiple samples of the various ochres were prepared, where possible, in order to assess the reproducibility of the procedures. Insufficient material from N5/24-6 (Puritjarra) and Wilgi Mia N-2b meant that only one sample was assessed from these sites. Blank samples, consisting of the Kartell tubes and cotton wool, were used throughout the measurement sequences, and where appropriate corrections were made to the magnetic parameters.

Magnetic parameters used

All of the techniques employed in this study are widely used in rock- and palaeomagnetic investigations and will only be briefly discussed below. More detailed information can be found in a variety of standard texts (e.g. Dunlop & Özdemir, 1997; Stacey & Banerjee, 1974; Thompson & Oldfield, 1986) or introductory papers such as Maher (1986). Table 1 gives a brief summary of all the magnetic parameters used.

Magnetic susceptibility. Magnetic susceptibility (χ) describes the magnetic response of a sample when exposed to a (generally weak) magnetic field. The induced magnetization is reversible, so no remanence is acquired. χ is mainly a function of the concentration and mineralogy of the ferrimagnetic (magnetite, maghemite, Fe-sulfides) minerals present, but can also depend on the strength of the applied magnetic field and the particle size distribution of the magnetic grains. In the absence of ferrimagnetic minerals χ can be due to antiferromagnetic (hematite, goethite),

paramagnetic (e.g., Fe-bearing silicates) or diamagnetic (e.g., quartz, calcite) minerals. Magnetic susceptibility is also dependent on sample size. Therefore it is customary to present susceptibility either as mass normalized susceptibility χ or volume normalized susceptibility κ . In SI units κ is a dimensionless quantity (m^3/m^3), while χ has the units of m^3/kg .

If susceptibility is measured in an alternating field it can be measured at different frequencies. Frequency dependent susceptibility (χ_{FD}) expresses the difference between susceptibility (χ_{lf}) measured at low frequency (often 470 Hz) and susceptibility (χ_{hf}) measured at high frequency (often 4.7 kHz), expressed as a percentage of χ_{lf} ($\chi_{FD} = (\chi_{lf} - \chi_{hf})/\chi_{lf} \times 100$). High values of χ_{FD} indicate the presence of very fine-grained metastable magnetic grains spanning the superparamagnetic (SP)—stable single domain (SSD) boundary (e.g. Eyre, 1997; Worm, 1998). For magnetite crystals this grain size boundary lies between 0.02–0.03 μm (Dunlop, 1973). These fine sizes are often diagnostic of secondary or authigenic magnetic minerals. Where susceptibility is mentioned in the text it always refers to a low frequency measurement.

χ was measured on a Bartington susceptibility meter, equipped with a dual frequency sensor and a Geofyzika Kappa Bridge KLY-2. χ_{FD} was measured on the Bartington susceptibility meter at frequencies of 470 Hz and 4.7 kHz and at 20 frequencies between 40 Hz and 4.0 kHz using a Lakeshore Series 7000 susceptometer. A logarithmic fit was used to reduce the data to two frequencies of 470 Hz and 4.7 kHz, which made it comparable to the Bartington results.

Isothermal Remanent Magnetization (IRM). IRM is the remanent magnetization acquired by a sample after

exposure to, and removal from, a steady (DC) magnetic field. IRM depends on the strength of the field applied, which is often denoted by a subscript. It is also a function of the magnetic mineralogy and grain size. The maximum remanence that can be produced in a sample is called Saturation Isothermal Remanent Magnetization (SIRM). IRM is often used as an indicator for the presence of ferrimagnetic minerals, but antiferromagnetic minerals, such as hematite and goethite are also capable of acquiring an IRM.

After a sample has acquired an IRM it is often possible to (partially) demagnetize the sample by exposing it to a magnetic field of reversed direction. Such a partial demagnetization can yield information about the ease of remanence acquisition, or the coercivity of a sample. The results are expressed as an S-ratio, for example,

$$S_{100} = \text{IRM}_{-100} / \text{SIRM},$$

where IRM_{-100} denotes an IRM acquired in a reversed field of 100 mT after SIRM acquisition. S-ratios can be used to gain information about the magnetic mineralogy (Bloemendal *et al.*, 1992). S-ratios close to +1.0 are indicative of ferrimagnetic minerals, while low S-ratios (<0.6 or even <0) are caused by the presence of antiferromagnetic minerals.

IRM acquisition curves track the acquisition of IRM in magnetic fields of increasing strength. They give information about the coercivity distribution of a sample, indicating at which fields a sample acquires its remanence. Coercivity spectra are obtained by taking the derivative of the acquisition curve. The spectra can be fitted using cumulative log Gaussian (CLG) distributions (Robertson & France, 1994; Stockhausen, 1998).

IRM was acquired by exposing the sample to a DC field of an electromagnet and measured using a Minispin fluxgate magnetometer and a cryogenic magnetometer (2G corp. model 760-R). CLGs were fitted to the gradient curves using a simple fitting program written in *Mathematica*.

Anhyseretic Remanent Magnetization (ARM). ARM is the remanence acquired by a sample when exposed to a small (50–100 μT) bias field, which is superimposed on a much stronger (peak field=70–200 mT) demagnetizing AF field. ARM can be highly sensitive to the presence of small single-domain (SD) grains, which for magnetite lies between 0.03 μm < d < 0.06 μm (Dunlop & Özdemir, 1997; Hunt *et al.*, 1995), but can also be influenced by magnetic interactions between magnetic particles (Sugiura, 1979; Yamazaki & Ioka, 1997). ARM was acquired in a peak AF field of 100 mT and a bias field of 50 μT and was measured using the 2G cryogenic magnetometer.

Hysteresis loops. Hysteresis loops describe the magnetic response of a sample while it is exposed to a

magnetic field. The shape of a hysteresis loop can be diagnostic of the mineralogy of the sample (e.g. Channell & McCabe, 1994; Tauxe *et al.*, 1996). Ferrimagnetic minerals tend to produce narrow loops, while the presence of antiferromagnetic minerals causes hysteresis loops to be wider. Hysteresis parameters can also be used to estimate magnetic grain size (e.g. Day *et al.*, 1977). When measuring a hysteresis loop the sample is exposed to a maximum field B_{max} and its magnetization (M) is measured as the field is reduced to zero and increased again in opposite direction all the way to $-B_{\text{max}}$. The remanence measured at zero field is equivalent to IRM mentioned before. The field B_C necessary to reduce the magnetization to zero is called the coercive force, and can be used to estimate the bulk coercivity of the sample. At high fields the curve $M(B)$ becomes linear and the increase in M is due to the presence of para- or diamagnetic minerals. This high field slope is known as highfield paramagnetic susceptibility. The saturation magnetization M_S of the sample can be calculated from a hysteresis loop by extrapolating the linear high-field part of the loop back to $B=0$. M_S is a function of all magnetic minerals (ferri- and antiferromagnetic) present in the sample.

We measured hysteresis loops in a maximum field of 1250 mT using a vibrating sample magnetometer (VSM) constructed at the Institute for Rock Magnetism. In addition we measured hysteresis loops with a maximum field of 5T using a Quantum Design MPMS-2 magnetic-properties measurement system, equipped with a superconducting magnet. These high fields were necessary to fully saturate most samples. Coercive force (B_C), saturation isothermal remanence (SIRM) and saturation magnetization (M_S) cited were obtained from the latter measurements.

Results and Discussion

The magnetic characteristics of the ochres and samples are listed in Table 2.

Reproducibility of results. The majority of the replicated samples resulted in similar values for the various magnetic properties measured. Subsets of all samples have been measured in two laboratories using a variety of equipment. Though there are some systematic differences between the two sets of measurements the results are very similar (Table 2). Variability is most pronounced in χ_{FD} measurements, due to the fact that the samples are very weak, and the measurements performed with the Bartington dual frequency sensor are less accurate than the measurements performed over a range of 20 frequencies using the Lakeshore susceptometer.

The samples from the Ulpunyali (MAS 1) site are an exception to the general trend of well-replicated samples. The duplicated unground versus ground

samples from this site show significant differences in their magnetic behaviour. The ground sample has higher susceptibility (4.16×10^{-7} vs. $2.16 \times 10^{-7} \text{ m}^3/\text{kg}$), a higher S-ratio (-0.77 vs. -0.88) and significantly higher frequency dependence of susceptibility (5.8% vs. 0.86%). These differences indicate the presence of a low coercivity ferrimagnetic component in the ground sample, which is absent in the unground specimen. These differences could be due to the natural variability of the sample, but replicated samples from this site, taken on a different occasion, are very similar to the unground sample, and it is likely that the ground sample was contaminated during the grinding process.

To further evaluate the validity of our approach, however, it is necessary to study the variability of magnetic properties for samples from a given site in greater detail. In this way the variation of several samples from the same source could be assessed, however restrictions on access and availability of samples does not allow this in all cases.

Magnetic properties of ochres and the sediment matrix. The magnetic mineralogy of the ochres, as already suggested by the color of the samples, consists mainly of the antiferromagnetic minerals hematite (red and purple samples) and goethite (yellow samples).

The magnetic properties of the sediment matrix are caused by a combination of ferrimagnetic (magnetite or maghemite) and antiferromagnetic (hematite) minerals. These differences in mineralogy mean that the sediment matrix (N13-N-95) is easily distinguished from the archaeological ochres at this site (e.g. N5/24-6). The sediment matrix shows high values of magnetic susceptibility, but relatively low values for IRM (Figure 2), resulting in a low IRM/ χ ratio (8 kA/m). Ochre samples, on the other hand, display a range of susceptibilities combined with disproportionately high values for IRM, causing high ratios of IRM/ χ between 77 kA/m and 330 kA/m.

Hysteresis loops also reflect the differences in mineralogy between the sediment sample and the archaeological ochres (Figure 3). While the sediment matrix is characterized by an almost reversible loop, characteristic of magnetically soft ferrimagnetic minerals, ochre samples display wide loops with large hysteresis. Loops for ochre samples are generally not closed, indicating that they were not saturated in the maximum applied field of 1250 mT. Further characterization revealed that most red ochres are only saturated in magnetic fields above 3 T, while yellow ochres may not be saturated in a magnetic field of 5 T, the maximum field obtainable in our laboratory. Therefore, SIRM values have been calculated from hysteresis loops measured in a maximum field of 5.0 T.

The hysteresis loops (Figure 3) are also useful for a qualitative characterization of the ochres. Constricted loops (Bookartoo and Ulpunyali MAS1 ground) indicate the presence of two or more coercivity fractions (e.g. Tauxe *et al.*, 1996), while samples consisting only

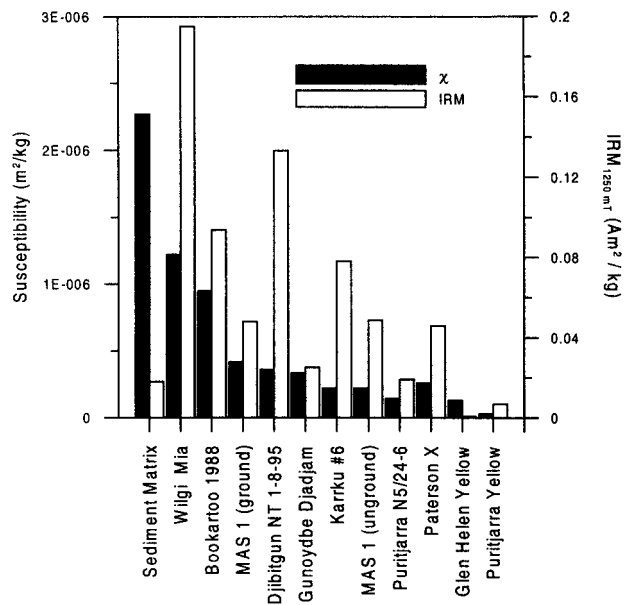


Figure 2. Magnetic susceptibility χ and SIRM values (max. field 5T) for all samples. Samples are arranged in order of decreasing χ . SIRM does not follow this systematic decrease because it is carried mostly by antiferromagnetic minerals, while χ mainly reflects the presence of ferrimagnetic minerals.

of antiferromagnetic minerals show thick, potbellied loops (Puritjarra yellow ochre and Ulpunyali MAS1 unground).

IRM acquisition curves show that ochre samples acquire most of their magnetic remanence in fields larger than 100 mT, while the sediment matrix acquired most of its remanence in fields between 10 and 75 mT (Figure 4). The Bookartoo sample displayed a distinct increase in remanence at low fields (10–125 mT), combined with a second increase at higher fields (>300 mT), again reflecting the presence of two coercivity phases, a magnetically soft phase carried by ferrimagnetic minerals, and a magnetically hard phase due to antiferromagnetic minerals. Other samples (e.g. Ulpunyali) show only an increase in remanence at fields larger than 200 mT, caused by antiferromagnetic hematite. A yellow ochre sample (Glen Helen in Figure 4a) shows its main increase in remanence at even higher magnetic fields (>500 mT) and there is no indication of the sample becoming saturated. This extremely hard behaviour is caused by the presence of antiferromagnetic goethite.

The gradient $d\text{IRM}/d\text{B}$ of the IRM acquisition curves (Figure 4b–d) can be used to further characterize the coercivity spectra of the ochres. The gradient data (solid circles in Figure 4c–d) are fitted to Cumulative Log Gaussian (CLG) distributions (Robertson & France, 1994). Figure 4b–d illustrate the range of coercivity distributions encountered in the sample set. The IRM acquisition curve of the sediment matrix is dominated by a low-coercivity component centred around a peak field of 15 mT. A high coercivity

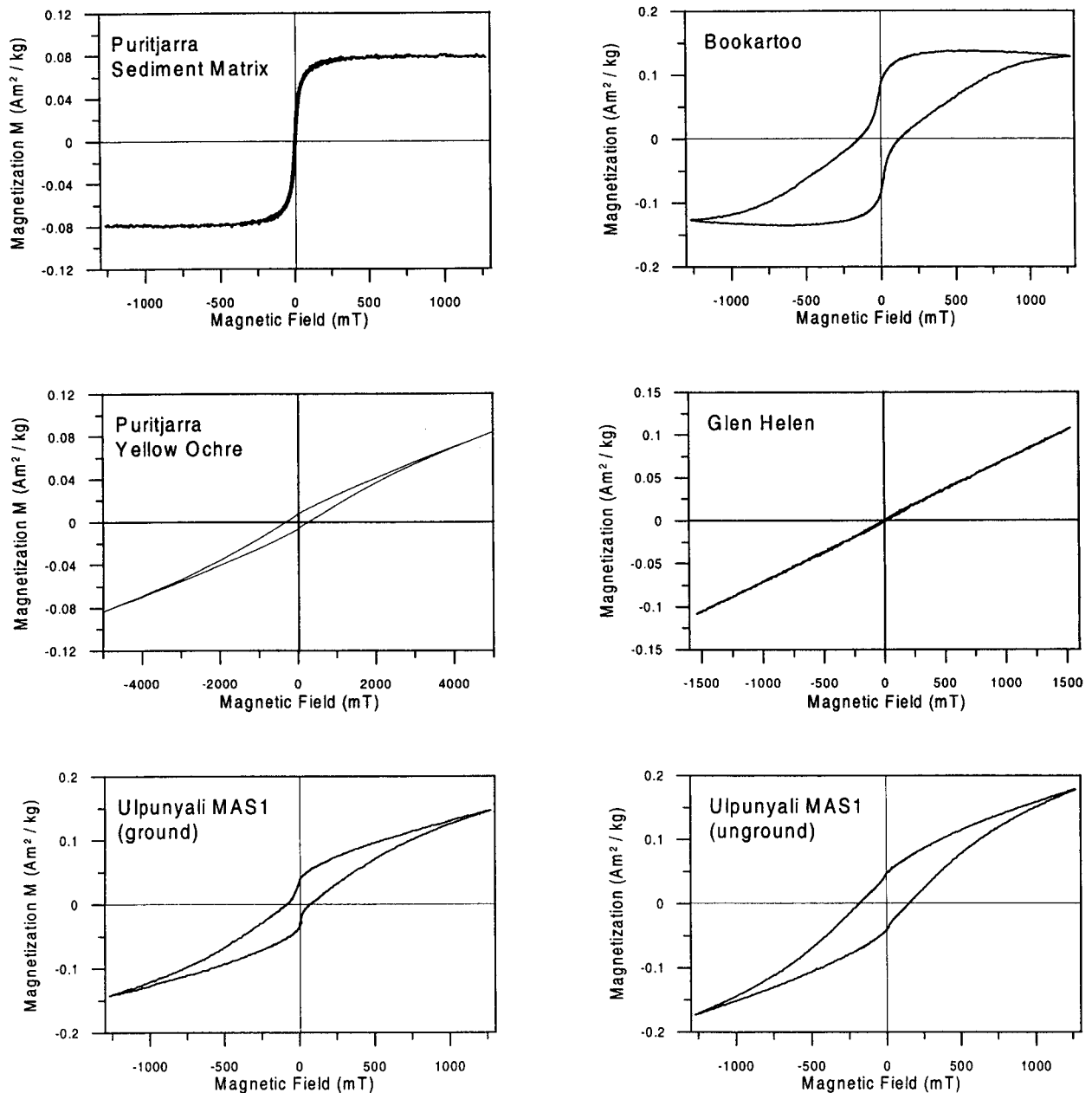


Figure 3. Hysteresis loops illustrating the range of shapes encountered in the sample set. Low coercivity ferrimagnetic minerals tend to produce narrow loops, while high coercivity antiferromagnetic minerals are responsible for the open loops. Hysteresis loops constricted near the origin indicate the presence of two coercivity components, and clearly differentiate the ground and unground sample from Ulpunyali.

component, centred on fields of 300–500 mT, is present and dominates the magnetic properties of all ochres. The low-coercivity (magnetically soft) component is due to the presence of ferrimagnetic magnetite or maghemite, while the high coercivity (magnetically hard) component is caused by the presence of antiferromagnetic hematite.

The method fails for the Glen Helen yellow ochre, shown in Figure 4a. Yellow ochres cannot be saturated in this experiment and no CLG can be reliably fitted to the data. The amount of remanence gained by

each coercivity component is proportional to the area under the respective CLG, and, since all curves are plotted on a semilogarithmic scale, all ochres are dominated by their high coercivity component. It should also be kept in mind that the amount of remanence gained by a mineral is also dependent on its saturation magnetization M_S . Magnetite and maghemite are characterized by high values of M_S (480–380 kA/m), while M_S is orders of magnitude lower for hematite (2.5 kA/m) and goethite (~ 2 kA/m) (Dunlop & Özdemir, 1997). Therefore, even though

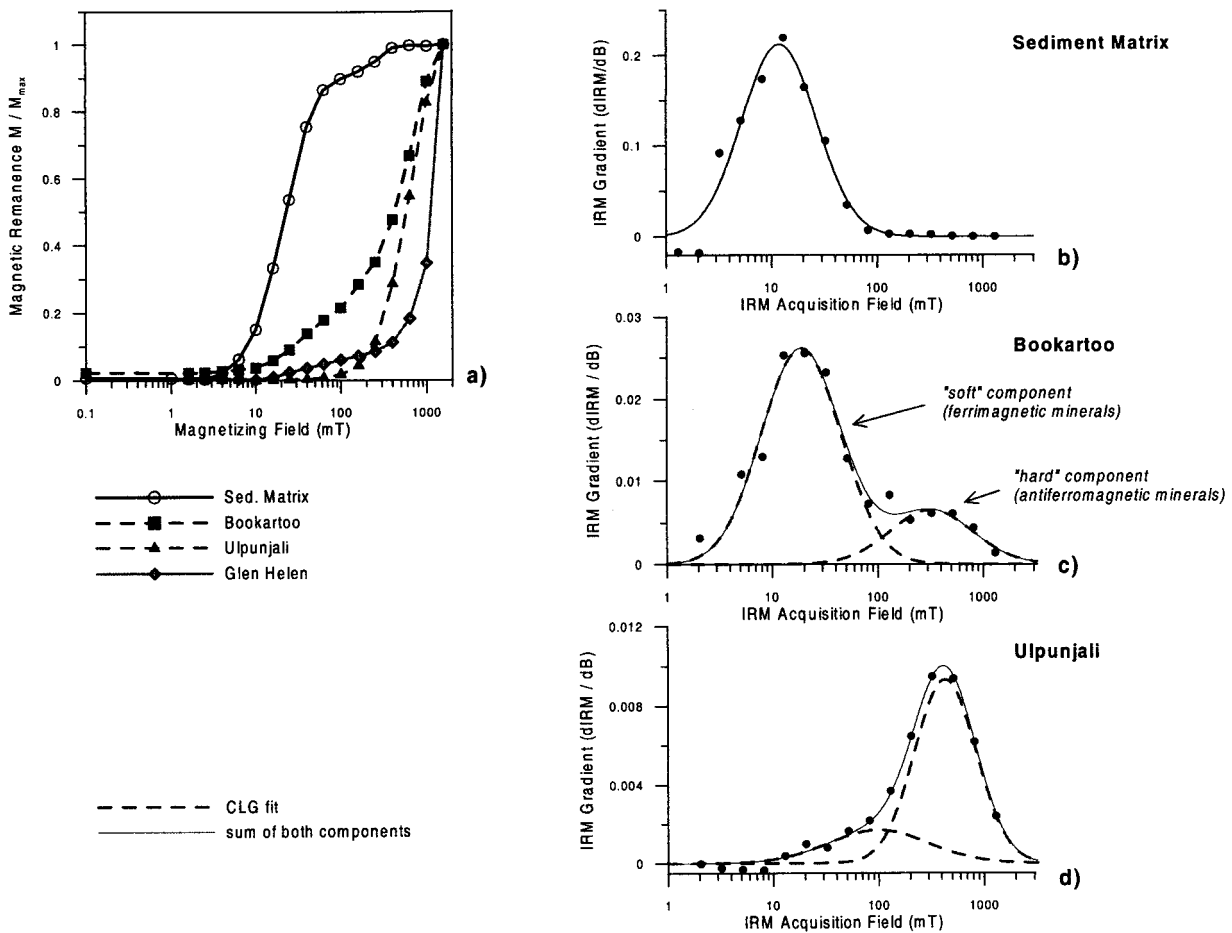


Figure 4. IRM acquisition for various samples. (a) IRM acquisition curves for a range of samples plotted on a semi logarithmic scale. (b)–(d) Coercivity spectra derived from the IRM acquisition curves shown in Figure 3a. Cumulative log Gaussian distributions (dashed grey lines) are fitted to the gradient of the IRM acquisition curve (solid circles). The result of CLG fits is shown in the solid line. (b) The sediment matrix is dominated by one low coercivity component with a peak near 15 mT. (d) The ochre from Ulpunjali (unground) is best fitted with a high coercivity component with a peak field of 340 mT. (c) Some ochres are composed of two coercivity components, resulting in two peaks in the coercivity spectra. The yellow ochres (e.g. Glen Helen in a) could not be saturated in a 1.6 T field and cannot be fitted using CLGs.

Figure 4b–d show distinct ferrimagnetic components, the magnetic mineralogy of all ochre samples and, though to a lesser degree, the sediment matrix, consists almost entirely of antiferromagnetic minerals.

Figure 5 presents a summary of coercivity spectra for all samples (except yellow ochres). In this figure a coercivity components peak field is marked as a darkened box and the tone of the box indicates how much this component contributes to the remanence of the sample, where a darker tone represents a high contribution. The samples are again arranged in order of decreasing magnetic susceptibility and it becomes evident that samples that have high values of χ are influenced by a soft coercivity component.

S-ratios also reflect the dominance of antiferromagnetic minerals in the ochre samples (Figure 6). S-ratios are extremely low (<0) for all ochres and the influence of ferrimagnetic minerals is visible in samples with high susceptibility, which have higher S-ratios. The

sediment matrix shows an S-ratio of 0.8, consistent with its large ferrimagnetic component.

ARM measurements were performed on all ochres prior to IRM acquisition. The results are listed in Table 2. The high coercivities of the samples, means however that the ARM measurements are not interpretable in terms of grain size or particle-interactions. (Most ARMs are acquired in an alternating peak field of 100 mT which is not high enough to significantly affect most tested ochres.)

Values for frequency dependent susceptibility (χ_{FD}) are also listed in Table 2. Figure 7 graphs χ_{FD} versus $SIRM/\chi$, showing how superparamagnetic (SP) grains, as estimated by χ_{FD} , lead to high values of χ and reduce $SIRM/\chi$ as they do not affect SIRM. This results in the negative correlation between the two parameters. This relative increase in χ is not constrained to samples that have a sizeable ferrimagnetic component, so at least part of the hematite must be in

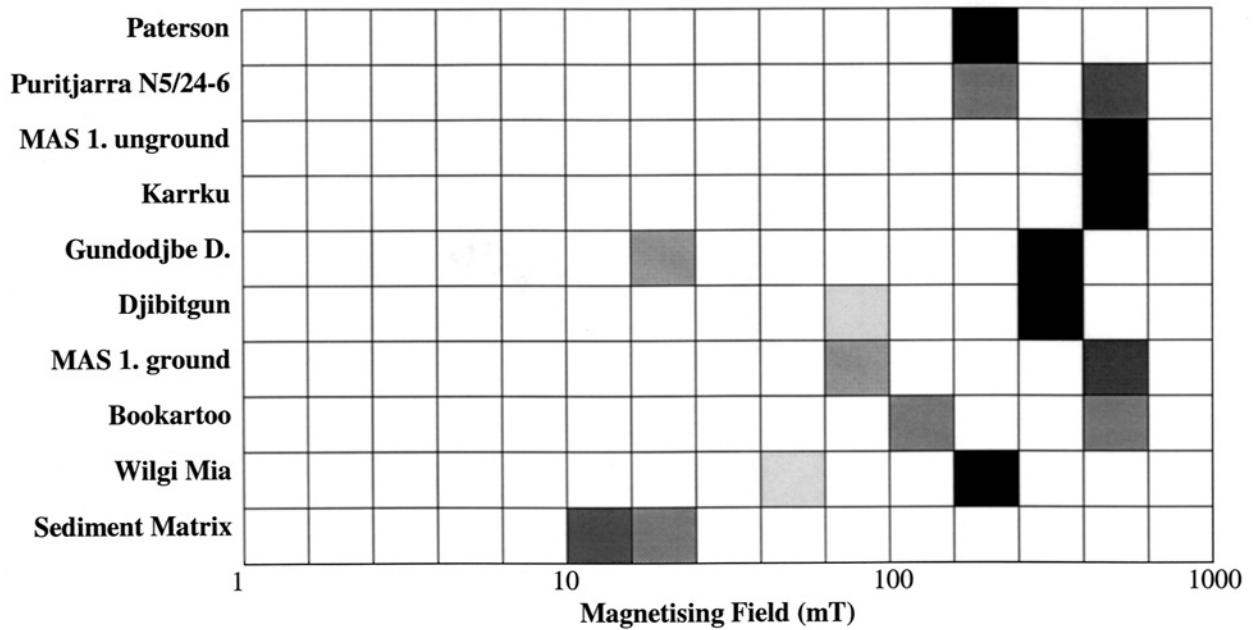


Figure 5. Location of main (black) and secondary (light grey) spectral peaks for all red ochres and the Puritjarra sediment matrix.

an ultra fine SP state ($d < 0.03 \mu\text{m}$). The presence of this ultra fine component is consistent with the sedimentary origin of these ochres (Smith & Pell, 1997).

Magnetic characterization of red ochres. From the results presented it is evident that magnetic properties can be used as a tool to distinguish ochres of varying

provenance. In general changes in magnetic properties can be due to subtle changes in abundance, mineralogy or particle-size distribution of magnetic minerals.

Among the parameters that are good indicators for the abundance of magnetic minerals are magnetic susceptibility (χ), SIRM and saturation magnetization (M_s). Figure 2 shows the large differences in χ and SIRM for the studied sample set. Ochres from Wilgi Mia, Bookartoo and Djibitgun, for example are much

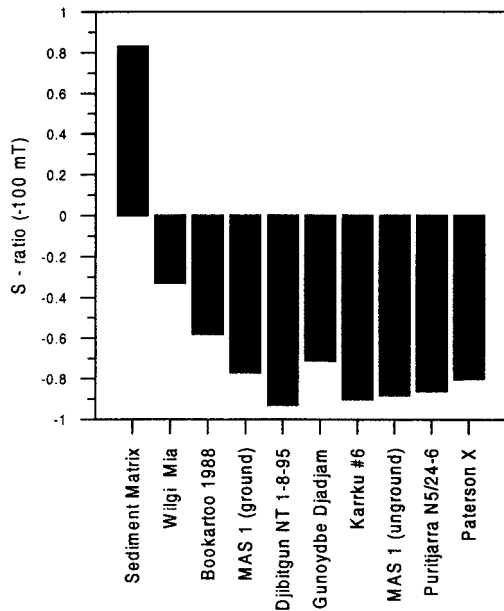


Figure 6. S-ratios (measured in “saturating” field of 1000 mT and a backfield of 100 mT) for all samples. Samples are arranged in order of decreasing magnetic susceptibility indicating that high χ values correlate with high S-ratios and the presence of a low coercivity (secondary) component. Negative S-ratios indicate that the sample is dominated by antiferromagnetic minerals.

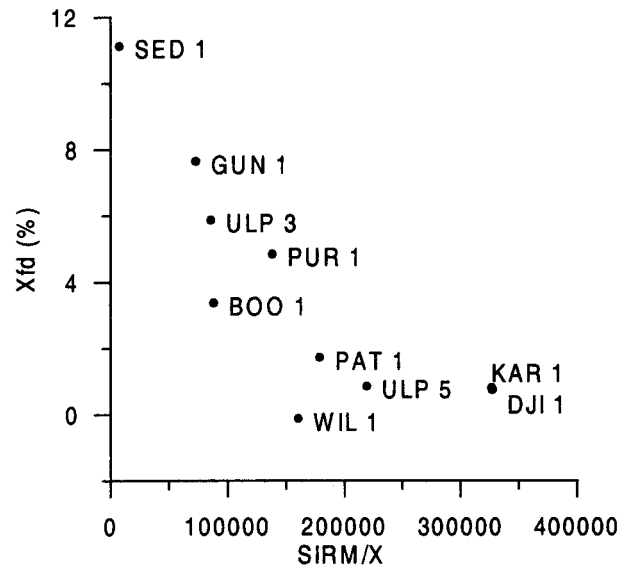


Figure 7. Scatterplot of frequency dependent susceptibility χ_{FD} versus $SIRM/\chi$. High values of χ_{FD} are due to the presence of ultrafine-grained, superparamagnetic (SP) magnetic minerals. These grains contribute to χ , but do not affect SIRM, leading to a negative correlation between the two parameters.

Table 3. Results of the squared Euclidean distance analyses (distance is small for cases that are similar)

Sample	Run 1		Run 2		Run 3		Average	
	PAT X	N5/24-6	PAT X	N5/24-6	PAT X	N5/24-6	PAT X	N5/24-6
Wilgi Mia	0.731	1	0.721	1	0.792	0.988	0.75 ± 0.03	0.996 ± 0.006
Bookartoo	0.184	0.275	0.206	0.295	0.216	0.319	0.20 ± 0.01	0.30 ± 0.02
Ulpunyali (unground)	0.0179	0.08	0.0202	0.0886	0.0187	0.012	0.019 ± 0.001	0.06 ± 0.03
Djibitgun	0.16	0.338	0.157	0.354	0.172	0.305	0.163 ± 0.006	0.33 ± 0.02
Gunoydbe Djadjam	0.143	0.0532	0.183	0.0686	0.0125	0.0341	0.11 ± 0.07	0.05 ± 0.01
Karrku	0.0559	0.169	0.0663	0.198	0.07	0.133	0.064 ± 0.006	0.17 ± 0.03
Puritjarra N5/24-6	0.0573	—	0.0697	—	0.0245	—	0.05 ± 0.02	—
Paterson X	—	0.0573	—	0.0697	—	0.0245	—	0.05 ± 0.02

Run 1 refers to an analyses which uses χ , SIRM, M_s , H_C and S-ratios. For Run 2 dissimilarities were calculated ignoring M_s , while Run 3 uses only χ , SIRM, H_C and S-ratios.

more magnetic than ochres from the Gunoydbe Djadjam or Puritjarra sites.

Differentiating between different mineralogies is possible with parameters that are mainly sensitive to changes in coercivity. S-ratios and IRM acquisition curves can be used to distinguish between low coercivity minerals such as magnetite and high coercivity minerals such as hematite and goethite. S-ratios and IRM acquisition curves indicate the presence of a small amount of magnetite or maghemite in some ochre samples (Wilgi Mia, Bookartoo, Ulpunyali), while others (Paterson, Puritjarra, Karrku) are free of these impurities.

Grain size dependent parameters, such as χ_{FD} , but also SIRM/ χ (Figure 7) show that some samples contain a significant extremely fine-grained superparamagnetic fraction (Gunoydbe Djadjam, Puritjarra).

Magnetic characterization of yellow ochres. The two yellow ochre samples (Puritjarra Yellow and Glen Helen) show significant differences in concentration and coercivity dependent parameters. Concentration dependent parameters, such as χ and IRM are low compared to red ochres (Figure 2), due to the low saturation magnetization and extremely high coercivity of goethite. The hysteresis loop (Figure 3) and the IRM acquisition curve (Figure 4a) of the yellow ochre from Puritjarra are typical for a goethite dominated sample. The hysteresis loop is barely closed in a magnetic field of 4 T and the IRM acquisition curve shows that no onset of saturation occurs below 1.6 T.

The Glen Helen sample is dominated by a paramagnetic ore component, leading to a straight, reversible hysteresis loop (Figure 3). Calculation of the paramagnetic susceptibility χ_p yields a value of $8.66 \times 10^{-8} \text{ m}^3/\text{kg}$. This indicates that approximately two-thirds of the susceptibility of this sample is caused by the presence of paramagnetic minerals, such as iron-bearing clays.

Due to our limited sample set it is impossible to say whether the range of these observations is fairly typical and whether they can be used to identify yellow ochres.

Provenancing of the ochres of unknown source. The magnetic characteristics of the ochres of unknown source (Paterson X, Puritjarra N5/24-6) can provide clues to their source. Here the unsourced ochres are compared to the known ochre quarries by examining the statistical distance (or dissimilarity) between them. The ground Ulpunyali sample was excluded from this analysis due to the suspected contamination. The dissimilarity coefficient was calculated using squared Euclidean distance after transforming the data so that all variables ranged from -1.0 to $+1.0$. We used several combinations of magnetic parameters, and the results of these comparisons are shown Table 3. The results of the comparison using the entire set of parameters is shown as run 1 in Table 3. This selection biases towards concentration dependent parameters ($n=3$ vs. $n=2$ for coercivity, vs. $n=1$ for grain size), so we repeated our analysis using only χ and IRM (Table 3, run 2) and finally, only using χ , IRM, S_{100} and H_C (Table 3, run 3). The results of this comparison between the unsourced and the known ochre quarries are summarized in Figure 8.

The Paterson sample has very similar magnetic properties to samples from Ulpunyali (unground), Puritjarra and Karrku, while it is quite different from samples from Wilgi Mia, Bookartoo and Djibitgun. The magnetic properties of the Puritjarra sample (N5/24-6) are similar to those from Ulpunyali, Paterson and Gunoydbe Djadjam, while they have less in common with samples from Wilgi Mia, Djibitgun and Bookartoo.

This analysis largely concurs with the conclusions drawn by Smith & Pell (1997), based on $\delta^{18}\text{O}$ analyses. Both conclude that Bookartoo is an unlikely source for the two ochre samples, which are more likely to come from Puritjarra or Karrku. Magnetic properties, however, cannot reliably distinguish between the two unknown samples themselves, and the claim made by Smith & Pell (1997) that both samples are unlikely to come from the same source cannot be verified.

The results of the statistical analyses are also consistent with IRM acquisition spectra summarized in

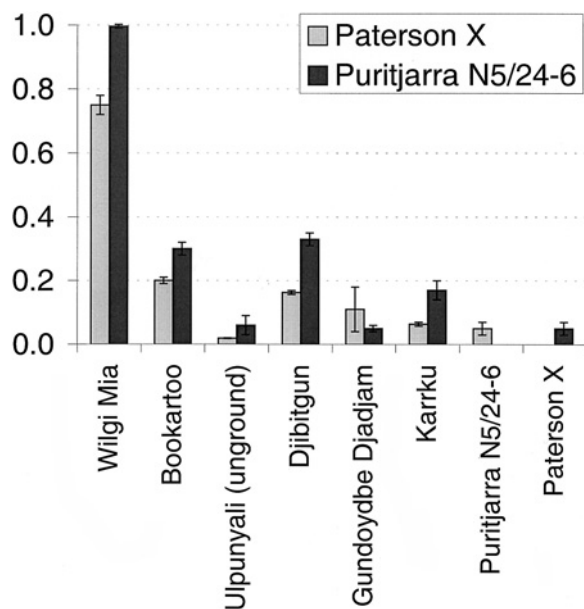


Figure 8. Summary of the squared Euclidean distance analyses for the unsourced samples, Paterson X and Puritjarra N5/24-6. A larger distance measure means that the samples are less alike, hence on the basis of the magnetic measurements Paterson X is most like the unground Ulpunyali sample and the Puritjarra sample N5/24-6 is most like Gundoydbe Djadjam.

Figure 4. The coercivity of the Wilgi Mia sample is too low to explain the behaviour of the samples from Paterson and Puritjarra N5/24-6. Bookartoo also has a low coercivity component that makes it unlike the unknown samples.

Conclusions

The magnetic properties of the studied samples are dominated by the antiferromagnetic magnetic minerals hematite (red ochres) and goethite (yellow ochres) with only trace amounts of ferrimagnetic minerals such as magnetite or maghemite. In the case of the Puritjarra excavations, and probably for most central Australian sediment, this allows the distinction of ochre samples from the surrounding matrix, which is magnetically dominated by ferrimagnetic minerals.

The red ochres show distinctive variations in the concentration, particle-size and trace amounts of maghemite, which allows for their magnetic differentiation. Useful parameters for such studies are magnetic susceptibility (χ), frequency dependent susceptibility (χ_{FD}), isothermal remanent magnetization (IRM), IRM acquisition, S-ratios and hysteresis loops. All these measurements are fast, non-destructive, very sensitive and allow for the characterization of small amounts of sample (<1 g). Anhysteretic remanent magnetization (ARM) is likely to be less useful due to the high coercivity of the studied minerals, which makes ARM acquisition difficult.

A multi-parameter approach using distance measures has also facilitated determination of the likely provenance of ochres of unknown source. However, more replicates from each of the ochre sources are warranted to further assess the variations within sites, and hence to provide a firmer basis for provenancing. Similarly, other magnetic parameters, such as the mapping of mineralogical phase transitions at low temperatures (e.g. Morin, 1950) or the determination of Curie temperatures, are likely to provide more subtle magnetic characterization and hence better differentiation.

The magnetic characterization of the archaeological ochre N5/24-6 suggests Ulpunyali, Gundoydbe Djadjam or the Karrku quarry as likely sources. Paterson X has a high degree of similarity to the Ulpunyali and Karrku sources. These results are in accordance with those by Smith & Pell (1997), suggesting that magnetic parameters may be a useful and perhaps simpler method of provenancing archaeological ochres.

Acknowledgements

Dr Barry Perczuk in the School of Physics, UNSW kindly granted access to the electro-magnet used for the original IRM determinations. Steve Filan, School of Geography, UNSW provided statistical advice. Mike Jackson from the Institute of Rock Magnetism (IRM), UMN, kindly provided advice and discussions. The IRM is funded by the W. M. Keck Foundation, the National Science Foundation's Earth Science Division's Instrumentation and Facilities Program and the University of Minnesota.

References

- Bloemendal, J., King, J. W., Hall, F. R. & Doh, S.-H. (1992). Rock magnetism of Late Neogene and Pleistocene deep-sea sediments: Relationship to sediment source, diagenetic processes, and sediment lithology. *Journal of Geophysical Research* **97**, 4361–4375.
- Channell, J. E. T. & McCabe, C. (1994). Comparison of magnetic hysteresis parameters of unremagnetized and remagnetized limestones. *Journal of Geophysical Research* **99**(B3), 4613–4623.
- Clarke, J. (1976). Two Aboriginal rock art pigments from Western Australia; their properties, use and durability. *Studies in Conservation* **21**, 134–142.
- Clarke, J. & North, N. (1991). Pigment composition of post-estuarine rock art in Kakadu National Park. In (C. Pearson & B. K. Swartz, Eds) *Rock Art and Posterity: Conserving, Managing, and Recording Rock Art*. Occasional AURA Publication 4, Melbourne, Australian Rock Art research Association, pp. 80–87.
- David, B., Clayton, E. & Watchman, A. (1993). Initial results of PIXE analysis on Northern Australian ochres. *Australian Archaeology* **36**, 50–57.
- David, B., Watchman, A., Goodall, R. & Clayton, E. (1995). The Maytown ochre source. *Memoirs of the Queensland Museum* **38**, 441–445.
- Davidson, D. S. (1952). Notes on the pictographs and petroglyphs of Western Australia and a discussion on their affinities with appearances elsewhere on the continent. *Proceedings of the American Philosophical Society* **96**, 82–84.

- Day, R., Fuller, M. & Schmidt, V. A. (1977). Hysteresis properties of titanomagnetites: Grain-size and compositional dependence. *Physics of the Earth and Planetary Interiors* **13**, 260–267.
- Dearing, J. A. & Flower, R. J. (1982). The magnetic susceptibility of sedimenting material trapped in Lough Neagh, Northern Ireland and its erosional significance. *Limnology and Oceanography* **17**, 969–975.
- Dunlop, D. J. (1973). Superparamagnetic and single-domain threshold sizes in magnetite. *Journal of Geophysical Research* **78**, 1780–1793.
- Dunlop, D. J. & Özdemir, Ö. (1997). *Rock Magnetism, Fundamentals and Frontiers*. Cambridge, New York: Cambridge University Press.
- Elias, M. (1982). *Belele, Western Australia, 1:250,000 Geological Series—Explanatory Notes, Sheet SG50-11*. Perth, WA: Geological Survey of Western Australia.
- Eyre, J. (1997). Frequency dependence of magnetic susceptibility for populations of single-domain-grains. *Geophysical Journal International* **129**, 209–211.
- Fullager, R. L. K., Price, D. M. & Head, L. M. (1996). Early human occupation of northern Australia: archaeology and thermoluminescence dating of Jinnium rock-shelter, Northern Territory. *Antiquity* **70**, 751–773.
- Goodall, R., David, B. & Bartley, J. (1996). Non-destructive techniques for the analysis and characterisation of pigments from archaeological sites: The case of Fern Cave. In (S. Ulm, I. Lilley & A. Ross, Eds) *Australian Archaeology '95: Proceedings of the 1995 Australian Archaeological Association Annual Conference*. Brisbane: University of Queensland, St Lucia, pp. 183–187.
- Hunt, C. P., Moskowitz, B. M. & Banerjee, S. K. (1995). Magnetic properties of rocks and minerals. In (T. J. Ahrens, Ed.) *Rock Physics and Phase Relations. A Handbook of Physical Constants*, AGU Reference Shelf, pp. 189–204.
- Keeling, J. L. (1984). Bookartoo ochre deposit. Report Book No. 831, DME 36/61. Adelaide: Department of Mines and Energy (South Australia).
- Maher, B. A. (1986). Characterization of soils by mineral magnetic measurements. *Physics of the Earth and Planetary Interiors* **42**, 76–92.
- Maher, B. A. & Thompson, R. (1992). Paleoclimatic significance of the mineral magnetic record of the Chinese loess and paleosols. *Quaternary Research* **37**, 155–170.
- Morin, F. J. (1950). Magnetic susceptibility of α -Fe₂O₃ and α -Fe₂O₃ with added titanium. *Journal of Physics* **3**, 819–820.
- Munsell (1994). *Munsell Color Charts*. Revised Edition. New York: Munsell Color, New Windsor.
- Oldfield, F. (1988). Magnetic and element analysis of recent lake sediments from the highlands of Papua New Guinea. *Journal of Biogeography* **15**, 529–553.
- Oldfield, F. (1991). Environmental magnetism: A personal perspective. *Quaternary Science Reviews* **10**, 73–85.
- Oldfield, F., Tolonen, K. & Thompson, R. (1981). History of particulate atmospheric pollution from magnetic measurements in dated Finnish peat profiles. *Ambio* **10**, 185–188.
- Peterson, N. & Lampert, R. (1985). A Central Australian ochre mine. *Records of the Australian Museum* **37**, 1–9.
- Robertson, D. J. & France, D. E. (1994). Discrimination of remanence-carrying minerals in mixtures, using isothermal remanent magnetization acquisition curves. *Physics of the Earth and Planetary Interiors* **82**, 223–234.
- Rummery, T. A. (1983). The use of magnetic measurements in interpreting the fire histories of lake basins. *Hydrobiologia* **103**, 53–58.
- Sagona, A. (Ed.) (1994). *Bruising the Red Earth: Ochre Mining and Ritual in Aboriginal Tasmania*. Melbourne: Melbourne University Press.
- Smith, M. A. (1987). Pleistocene occupation in arid Central Australia. *Nature* **328**, 710–711.
- Smith, M. A. & Fankhauser, B. (1996). An archaeological perspective on the geochemistry of Australian red ochre deposits: Prospects for fingerprinting major sources. Report to the Australian Institute of Aboriginal and Torres Strait Islander Studies, Canberra.
- Smith, M. A. & Pell, S. (1997). Oxygen-isotope ratios in quartz as indicators of the provenance of archaeological ochres. *Journal of Archaeological Science* **24**, 773–778.
- Smith, M. A., Prescott, J. R. & Head, M. J. (1997). Comparison of ¹⁴C and luminescence chronologies at Puritjarra rock shelter, Central Australia. *Quaternary Geochronology (Quaternary Science Reviews)* **16**, 299–320.
- Smith, M. A., Fankhauser, B. & Jercher, M. (1998). The changing provenance of red ochre at Puritjarra rock shelter, Central Australia: Late Pleistocene to present. *Proceedings of the Prehistoric Society* **64**, 275–292.
- Stacey, F. D. & Banerjee, S. K. (1974). *The Physical Principles of Rock-magnetism*. Amsterdam: Elsevier.
- Stockhausen, H. (1998). Some new aspects for the modeling of isothermal remanent magnetization acquisition curves by cumulative log Gaussian functions. *Geophysical Research Letters* **25**(12), 2217–2020.
- Sugiura, N. (1979). ARM, TRM and magnetic interactions: Concentration dependence. *Earth and Planetary Science Letters* **42**, 451–455.
- Tauxe, L., Mullender, T. A. T. & Pick, T. (1996). Potbellies, wasp-waists, and superparamagnetism in magnetic hysteresis. *Journal of Geophysical Research* **101**, 571–583.
- Thompson, R. & Oldfield, F. (1986). *Environmental Magnetism*. London: Allen and Unwin.
- Thompson, R., Battarbee, R. W., O'Sullivan, P. E. & Oldfield, F. (1975). Magnetic susceptibility of lake sediments. *Limnology and Oceanography* **20**, 687–698.
- Worm, H.-U. (1998). On the superparamagnetic-stable single domain transition for magnetite, and frequency dependence of susceptibility. *Geophysical Journal International* **133**, 201–206.
- Yamazaki, T. & Ioka, N. (1997). Cautionary note on magnetic grain-size estimation using the ratio of ARM to magnetic susceptibility. *Geophysical Research Letters* **24**, 751–754.
- Zhou, L. P., Oldfield, F., Wintle, A. G., Robinson, S. G. & Wang, J. T. (1990). Partly pedogenic origin of magnetic variations in Chinese loess. *Nature* **346**, 737–739.